The 17th European Conference on Circuit Theory and Design (an IEEE conference)
29 August – 1 September 2005, Cork, Ireland.

Modeling Finite-Memory Nonlinearity in Unit DAC Elements, Binary Storage Channels, and BPSK Data Channels

Jeffrey O. Coleman*

***Abstract*—Spectral shaping of quantization noise can allow a few (or one) oversampled D/A converters restricted to two output levels, *unit DAC elements*, to replace high-resolution converters. In high-resolution or high-speed settings however, even the performance of systems with only two output levels can be limited by conversion-circuit nonlinearities that introduce quantization-noise intermodulation products into the signal band through *nonlinear intersymbol interference* (ISI). Nonlinear ISI also affects the communication and magnetic storage of data. Here a simple but very general model structure for such binary-in, analog-out nonlinearities is proposed. Curiously, its structure is that of a convolutional coder whose output bits are separately LTI filtered before being finally summed to form the analog output. "The code" here can be chosen in a way that gives natural interpretations to those of its filter responses that are most likely to be significant.**

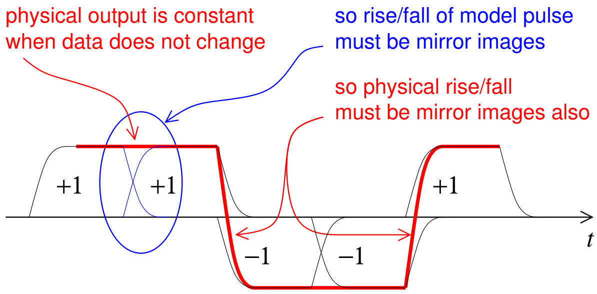

Figure 1: NRZ data with asymmetric transitions can never be expressed as $\sum_n x(n)\,h(t-nT)$, as ±1 binary data $x(n)$ LTI modulating a model pulse $h(t)$. Asymmetry implies nonlinearity.

1 INTRODUCTION

The success of single-bit $\Delta\Sigma$ modulation for D/A conversion is often ascribed to the inherent linearity of a two-level output. Two levels can always be expressed as deviations $\sigma \pm \delta$ from their average σ, so level errors yield at worst a DC offset and a gain error. But linearity disappears—see Fig. 1—when transitions are neither infinitely fast nor perfectly symmetric. The linearity of the two-level output circuit, the *unit DAC element*, is in fact a major issue when high-performance noise shaping has placed the signal band in a deep hole in the quantization-noise spectrum. *Nonlinear intersymbol interference* (ISI) raises the signal-band noise floor, sometimes dramatically, by adding intermodulation noise.

Nonlinear equalization of this type of interference has been studied for the magnetic storage channel [1, 2], and the nonlinear channel models used there provide the starting point for the present work. However, those models distribute the desired LTI response across many internal waveforms, so nonlinearities are represented by small deviations from desired responses. While suitable for extremely nonlinear magnetic-recording channels, a model less sensitive to errors is more appropriate when the system is nearly linear, so the present model incorporates a transformation that isolates both the LTI system component and the most-important nonlinear component, the transition asymmetry emphasized by Fig. 1.

There are other well-known approaches that superficially appear related. The model presented here is a special-case Wiener-Hammerstein system: a cascade of an LTI system, a memoryless nonlinearity, and another LTI system. However, the literature on such systems and on their identification universally posits scalar connections between the three subsystems, but here those connections are vector valued even though the system input and output are not. Further, positing ±1 binary input data here fixes the first two subsystems. Only the third need be estimated. The substantial complexities of Wiener-Hammerstein identification can be bypassed.

One oft-cited patent [4] addresses the nonlinearities inherent in quantized pulse-width modulation, in which preliminary $\Delta\Sigma$ noise shaping shifts much of the quantization noise out of the signal band. Nonlinear spreading of quantization noise into the signal band is the issue there as here. But the source of nonlinearity there is the ideal modulation process itself, not circuit imperfection, and the input to the nonlinearity is not binary.

Andersson *et al.* [3] use $\Delta\Sigma$-style noise shaping with a nonlinear DAC model in the shaping loop. But their DAC is a conventional high-resolution DAC, so they cannot take advantage of a binary input, the key here.

2 THE SIMPLE MODELS, STEP BY STEP

High-density disk tracks have been successfully equalized for reading [1] using the simple finite-memory nonlinear model of Fig. 2, a *RAM nonlinearity*. Here a real (it could be complex) output $y(n)$ is determined via a lookup table (RAM) addressed by a short-term input history. Passing the ±1 binary input stream $x(n)$ to a tapped delay line[1] creates that history, the vector

$$\mathbf{x}(n) = [\,x(n),\, x(n{-}1),\, x(n{-}2), \ldots,\, x(n{-}N{+}1)\,]^T.$$

* Naval Research Laboratory (http://www.nrl.navy.mil/), Radar Division, Signal Processing Theory & Methods Section. This work was supported by the NRL funding base and the Office of Naval Research (http://www.onr.navy.mil/). Author: http://alum.mit.edu/www/jeffc,

[1] Magnetic storage channels can be noncausal, so the "delay line" can differ from the causal form assumed here for simplicity of exposition.

Figure 2: RAM or lookup-table model of a finite-memory discrete-time nonlinearity from a binary input sequence $x(n)$ to a complex output sequence $y(n)$.

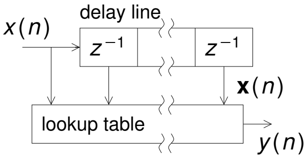

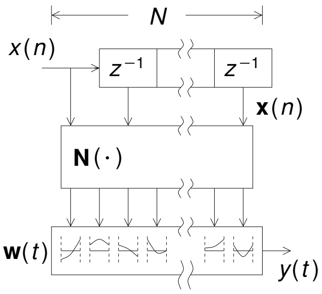

Figure 3: A generalizion of Fig. 2 to a continuous-time output. Here the nonlinearity $\mathsf{N}(\cdot)$ maps the 2^N distinct N-vector address inputs $\mathbf{x}(n)$ onto the 2^N distinct standard unit vectors $(0\ldots010\ldots0)^T$ of length 2^N. This unit vector selects a waveform segment from vector $\mathbf{w}(t)$ to be the output $y(t)$ in clock interval n.

Figure 4: Vector address $\mathbf{x}(n)$ here selects, through $\mathsf{N}(\cdot)$, a row of matrix $\mathbf{A}$ to output from the center block. The product with waveform vector $\mathbf{A}^{-1}\mathbf{w}(t)$ then contributes to output $y(t)$. Choosing matrix $\mathbf{A}$ well imparts meaning to elements of $\mathbf{A}^{-1}\mathbf{w}(t)$. Output content in some band of interest can be modeled by replacing $\mathbf{A}^{-1}\mathbf{w}(t)$ with a discrete-time vector signal $\mathbf{h}(n)$ and a bandlimited reconstruction filter $b(t)$.

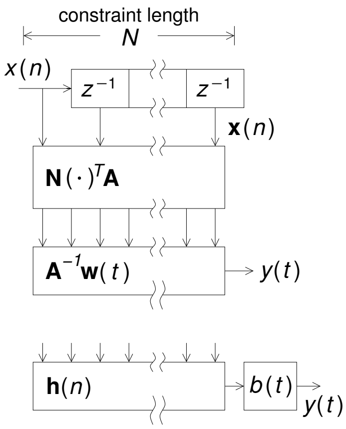

Multiple output values per clock interval can be obtained with multiple lookup tables [2], but a general continuous-time output waveform requires either an infinite number of such tables or some equivalent, such as shown in Fig. 3. Here the lookup table has been split into two parts. Following [2], binary N-vector $\mathbf{x}(n)$ addresses one of the length 2^N standard unit vectors $\widehat{e}_1,\ldots,\widehat{e}_{2^N}$, which is then output by nonlinearity $\mathsf{N}(\cdot)$. That standard unit vector then selects, via a dot product, one element of the length-2^N waveform vector $\mathbf{w}(t)$ to be the current clock interval's contribution to output

$$y(t) = \sum_n \mathsf{N}(\mathbf{x}(n))^T \mathbf{w}(t-nT). \qquad (1)$$

All elements of vector $\mathbf{w}(t)$ are supported on the same single clock interval, say $[\,0,T)$, so the shifting and summing simply stitches output segments together, end to end. Only one term of the sum is nonzero at a time.

The systems of Figs. 2 and 3 do not separate linear and nonlinear response components, but we can modify the Fig. 3 model to do so and to give nonlinear contributions an ordering roughly corresponding to importance.

If $2^N\times 2^N$ matrix $\mathbf{A}$ is nonsingular, then $\mathbf{A}\mathbf{A}^{-1}=\mathbf{I}$ can be inserted into (1) without harm, so we can write

$$y(t) = \sum_n [\mathsf{N}(\mathbf{x}(n))^T\mathbf{A}]\,[\mathbf{A}^{-1}\mathbf{w}(t-nT)].$$

We can realize $\mathsf{N}(\mathbf{x}(n))^T\mathbf{A}$ in the lookup operation by having address vector $\mathbf{x}(n)$ select a row of $\mathbf{A}$ to pass on rather than a standard unit vector. That row multiplies new waveform vector $\mathbf{A}^{-1}\mathbf{w}(t)$ to yield a component to be added to the output in the appropriate time slot. In simulation the $\mathbf{A}^{-1}\mathbf{w}(t)$ waveform vector can be synthesized from samples as shown in Fig. 4, where discrete-time vector $\mathbf{h}(n)$ has been designed so that

$$\mathbf{A}^{-1}\mathbf{w}(t) = \sum_n \mathbf{h}(n)\, b(t-nT).$$

with $b(t)$ some bandlimiting filter. Or more precisely, using Fourier-transformed quantities, $\mathbf{H}(fT)\,\mathrm{B}(f) = \mathbf{A}^{-1}\mathbf{W}(f)$ in the spectral region of interest. Here input and output-synthesis sample rates are identical at T^{-1}, but straightforward extension of the system to a higher output rate could increase output bandwidth if needed.

In proposing candidate matrices $\mathbf{A}$, we will consider the *constraint length* $N = 1,2,3$ cases separately before considering arbitrary N. The memoryless nonlinear map $\mathbf{x}(n) \mapsto \mathsf{N}(\mathbf{x}(n))^T\mathbf{A}$ will be given by tabulating the 2^N distinct $\big(\mathbf{x}(n)^T, \mathsf{N}(\mathbf{x}(n))^T\mathbf{A}\big)$ pairs. The second component of each pair is just a row of $\mathbf{A}$, so the table as a whole is a listing of $\mathbf{A}$. The entire purpose of the $\mathbf{A}$ and $\mathbf{A}^{-1}$ factors lies in the useful interpretations a well-chosen $\mathbf{A}$ matrix can impart to individual elements of waveform vector $\mathbf{A}^{-1}\mathbf{w}(t)$, so let us choose our first $\mathbf{A}$ to make the LTI component of the system explicit.

Nonlinearity Without Nonlinear Memory: If $N=1$ so that no z^{-1} delays appear in Fig. 4, we can use this:

$\mathbf{x}(n)^T$	$\mathsf{N}(\mathbf{x}(n))^T\mathbf{A}$
(-1)	$(1 \quad -1)$
$(\ \ 1)$	$(1 \quad\ \ 1)$

$$\mathbf{A}^{-1}\mathbf{w}(t) = \begin{bmatrix} c(t) \\ h(t) \end{bmatrix}$$

Here $x(n)=\pm 1$ contributes $c(t-nT)\pm h(t-nT)$ to output $y(t)$, so $h(t)$ is the bit response (impulse response) of an LTI system component. When $h(t)=0$ a periodic output results, independent of the input, so the nonlinearity characterized by $c(t)$ simply adds clock-harmonic spectral lines to the output.

Earlier we supposed $\mathbf{w}(t)$ to have support contained in one clock interval, perhaps $[0,T)$, but relaxing this to $[\,0,\infty)$ does not change the possible periodic output components, and it permits many more LTI system components. The model becomes more general. We continue to seek this sort of "free" generalization below.

The Minimal Nonlinear Memory: When Fig. 4 has $N=2$, or one z^{-1} delay, the table has four rows and its right side has four columns. The n dependence in the column headings is dropped for brevity, and the characters $\cdot\ +\ -$ represent 0, 1, and -1 respectively, Individual elements of $\mathbf{A}^{-1}\mathbf{w}(t)$ have supports contained in the intervals shown on the extreme right:

$\mathbf{x}^T$	$\mathbf{N}(\mathbf{x})^T\mathbf{A}$
$--$	$+--\cdot$
$+-$	$++-+$
$-+$	$+-++$
$++$	$+++\cdot$

$$\mathbf{A}^{-1}\mathbf{w}(t) = \begin{bmatrix} c(t) \\ h_0(t) \\ h_1(t) \\ a(t) \end{bmatrix} \quad \begin{matrix} [0,T) \\ [0,T) \\ [0,\infty) \\ [0,\infty) \end{matrix}$$

The $h_0(t)$ table column, the second on the right, is $+$ exactly when $x(n)$, the first column on the left is $+$, so $h_0(t)$ is effectively driven by $x(n)$. Likewise, the $h_1(t)$ column on the right matches the second column on the left, so $h_1(t)$ is effectively driven by $x(n-1)$. The two drive signals are the same except for a delay of T seconds, so subvector $\left[\begin{smallmatrix} h_0(t) \\ h_1(t) \end{smallmatrix}\right]$ represents an LTI impulse response $h_0(t)+h_1(t-T)$ driven by $x(n)$. Any causal LTI bit response can be represented then by some $\left[\begin{smallmatrix} h_0(t) \\ h_1(t) \end{smallmatrix}\right]$, and if the supports of $h_0(t)$ and $h_1(t)$ are confined respectively to the intervals shown the representation is unique. But the model is unchanged if we set $h_1(t)=0$ and put the entire LTI bit response in $h_0(t)$ and permit the latter support in $[0,\infty)$. We can drop both the zeroed third element from $\mathbf{A}^{-1}\mathbf{w}(t)$, now written as $\mathbf{h}(t)$, and the corresponding third column from $\mathbf{A}$:

$\mathbf{x}^T$	$\mathbf{N}(\mathbf{x})^T\mathbf{A}$
$--$	$+-\cdot$
$+-$	$+++$
$-+$	$+-+$
$++$	$++\cdot$

$$\mathbf{h}(t) = \begin{bmatrix} c(t) \\ h(t) \\ a(t) \end{bmatrix} \quad \begin{matrix} [0,T) \\ [0,\infty) \\ [0,\infty) \end{matrix}$$

As before, $c(t)$ models clock harmonics. The rightmost column drives $a(t)$ when $x(n-1)$ and $x(n)$ differ and so represents an asymmetric response to bit transitions.

A Little More Nonlinear Memory: Two z^{-1} delays in Fig. 4, or $N=3$, gives the table $2^N=8$ rows:

$\mathbf{x}^T$	$\mathbf{N}(\mathbf{x})^T\mathbf{A}$
$---$	$+---\cdot\cdot\cdot+$
$+--$	$++--+\cdot+\cdot$
$-+-$	$+-+-++\cdot\cdot$
$++-$	$+++-\cdot+++$
$--+$	$+--+\cdot++\cdot$
$+-+$	$++-+++\cdot+$
$-++$	$+-+++\cdot++$
$+++$	$++++\cdot\cdot\cdot\cdot$

$$\mathbf{A}^{-1}\mathbf{w}(t) = \begin{bmatrix} c(t) \\ h_0(t) \\ h_1(t) \\ h_2(t) \\ a_0(t) \\ a_1(t) \\ m_{02}(t) \\ m_{012}(t) \end{bmatrix} \quad \begin{matrix} \textit{support} \subset \\ [0,T) \\ [0,T) \\ [0,T) \\ [0,\infty) \\ [0,T) \\ [0,\infty) \\ [0,\infty) \\ [0,\infty) \end{matrix}$$

Here $c(t)$ is again one period of a clock-rate output component, but now subvector $[h_0(t),h_1(t),h_2(t)]^T$ represents LTI bit response $h_0(t)+h_1(t-T)+h_2(t-2T)$. Any causal response can be so represented, and if the supports of the $h_i(t)$ are contained as shown, the representation is unique. Equivalently, we can set $h_1(t)=h_2(t)=0$ and put the entire LTI bit response in $h_0(t)$, which is then allowed support in $[0,\infty)$. Similarly, the $a_0(t)$ table column is $+$ when $x(n)\neq x(n-1)$ and $\cdot$ otherwise, and the $a_1(t)$ table column is $+$ exactly when $x(n-1)\neq x(n-2)$. The drive signal to $a_1(t)$ is just the drive signal to $a_0(t)$ delayed by T, so asymmetry in the transition responses is modeled by $a_0(t)+a_1(t-T)$, and with the supports shown there is a unique $\left[\begin{smallmatrix} a_0(t) \\ a_1(t) \end{smallmatrix}\right]$ corresponding to an arbitrary causal response. We can set $a_1(t)=0$ and put the entire transition response in $a_0(t)$, which is then allowed support in $[0,\infty)$.

Six of the eight columns of $\mathbf{A}$ have now been chosen to give natural interpretations to the corresponding elements of waveform vector $\mathbf{A}^{-1}\mathbf{w}(t)$. The two remaining columns must be linearly independent of these six and of each other, but we are otherwise unconstrained in choosing them. Has a pattern been established in choosing the first six columns, one that we can now extend? Actually each $a_i(t)$ column is driven by a product of two input columns, and we can certainly regard each $h_i(t)$ column as driven by a "product" of one column only. We can even say that $c(t)$ is driven by an empty product, as the multiplicative identity is one. Only two possible products of columns remain unused, one of the first and third input columns and one of all three input columns, and these complete our table. We might expect that for a reasonable unit DAC element the $m_{02}(t)$ and $m_{012}(t)$ elements of $\mathbf{A}^{-1}\mathbf{w}(t)$ will be quite small, as they represent longer-memory nonlinear effects.

When zeroed elements of $\mathbf{A}^{-1}\mathbf{w}(t)$ and corresponding table columns are removed, the model simplifies to:

$\mathbf{x}^T$	$\mathbf{N}(\mathbf{x})^T\mathbf{A}$
$---$	$+-\cdot\cdot+$
$+--$	$++++\cdot$
$-+-$	$+-+\cdot\cdot$
$++-$	$++\cdot++$
$--+$	$+-\cdot+\cdot$
$+-+$	$+++\cdot+$
$-++$	$+-+++$
$+++$	$++\cdot\cdot\cdot$

$$\mathbf{h}(t) = \begin{bmatrix} c(t) \\ h(t) \\ a(t) \\ m_{02}(t) \\ m_{012}(t) \end{bmatrix} \quad \begin{matrix} [0,T) \\ [0,\infty) \\ [0,\infty) \\ [0,\infty) \\ [0,\infty) \end{matrix}$$

3 GENERALIZATION

Enumerate $0,1,2,\ldots,2^N-1$ in binary as the rows of a $2^N\times N$ label matrix $\mathbf{L}$ so that, for example, if $N=4$,

$$\mathbf{L}^T = \begin{bmatrix} \cdot\cdot\cdot\cdot\cdot\cdot\cdot\cdot++++++++ \\ \cdot\cdot\cdot\cdot++++\cdot\cdot\cdot\cdot++++ \\ \cdot\cdot++\cdot\cdot++\cdot\cdot++\cdot\cdot++ \\ \cdot+\cdot+\cdot+\cdot+\cdot+\cdot+\cdot+\cdot+ \end{bmatrix}.$$

Define map ϕ to return -1 or 1 according as its scalar argument is odd or even respectively and to operate elementwise on vectors and matrices. Initially, as in Fig. 5, label rows on the left with $\phi(\mathbf{L})$ and columns on the right with $\mathbf{L}^T$ and use Hadamard matrix $\phi(\mathbf{L}\mathbf{L}^T)$ as the table, so that each column on the right is the elementwise product of columns on the left identified by the former's vector label. This ensures that all 2^N distinct products of the N constituent factors are included.

$$\mathbf{L}^T = \begin{matrix} \cdot\cdot\cdot\cdot\cdot\cdot\cdot\cdot++++++++ \\ \cdot\cdot\cdot\cdot++++\cdot\cdot\cdot\cdot++++ \\ \cdot\cdot++\cdot\cdot++\cdot\cdot++\cdot\cdot++ \\ \cdot+\cdot+\cdot+\cdot+\cdot+\cdot+\cdot+\cdot+ \end{matrix}$$

$\mathbf{x}^T$	$\mathsf{N}(\mathbf{x})^T\mathbf{A}$
++++	++++++++++++++++
+++−	+−+−+−+−+−+−+−+−
++−+	++−−++−−++−−++−−
++−−	+−−++−−++−−++−−+
+−++	++++−−−−++++−−−−
+−+−	+−+−−+−++−+−−+−+
+−−+	++−−−−++++−−−−++
+−−−	+−−+−++−+−−+−++−
−+++	++++++++−−−−−−−−
−++−	+−+−+−+−−+−+−+−+
−+−+	++−−++−−−−++−−++
−+−−	+−−++−−+−++−−++−
−−++	++++−−−−−−−−++++
−−+−	+−+−−+−+−+−++−+−
−−−+	++−−−−++−−++++−−
−−−−	+−−+−++−−++−+−−+

Figure 5: The general construction of an $\mathbf{x} \mapsto \mathsf{N}(\mathbf{x})^T\mathbf{A}$ table begins with a Hadamard matrix with binary row and column labels.

$\mathbf{2}^T\boldsymbol{\ell}$	0	1	3	5	7	9	11	13	15
ℓ_1	·	+	+	+	+	+	+	+	+
ℓ_2	·	·	+	·	+	·	+	·	+
ℓ_3	·	·	·	+	+	·	·	+	+
ℓ_4	·	·	·	·	·	+	+	+	+
$\mathbf{x}^T$	$\mathsf{N}(\mathbf{x})^T\mathbf{A}$								
− − − −	+	−	·	·	+	·	+	+	·
+ − − −	+	+	+	+	·	+	·	·	+
− + − −	+	−	+	·	·	·	·	+	+
+ + − −	+	+	·	+	+	+	+	·	·
− − + −	+	−	·	+	·	·	+	·	+
+ − + −	+	+	+	·	+	+	·	+	·
− + + −	+	−	+	+	+	·	·	·	·
+ + + −	+	+	·	·	·	+	+	+	+
− − − +	+	−	·	·	+	+	·	·	+
+ − − +	+	+	+	+	·	·	+	+	·
− + − +	+	−	+	·	·	+	+	·	·
+ + − +	+	+	·	+	+	·	·	+	+
− − + +	+	−	·	+	·	+	·	+	·
+ − + +	+	+	+	·	+	·	+	·	+
− + + +	+	−	+	+	+	+	+	+	+
+ + + +	+	+	·	·	·	·	·	·	·

$\mathbf{h}(t) =$

	support $\subset$
$h_0(t)$	$[0,T)$
$h_1(t)$	$[0,\infty)$
$h_3(t)$	$[0,\infty)$
$h_5(t)$	$[0,\infty)$
$h_7(t)$	$[0,\infty)$
$h_9(t)$	$[0,\infty)$
$h_{11}(t)$	$[0,\infty)$
$h_{13}(t)$	$[0,\infty)$
$h_{15}(t)$	$[0,\infty)$

Figure 6: The general $\mathbf{x} \mapsto \mathsf{N}(\mathbf{x})^T\mathbf{A}$ map for constraint length N includes within it the maps for all shorter constraint lengths.

Several modest improvements are possible. Rather than associate columns $\begin{smallmatrix}+\\ \cdot\\ \cdot\\ \cdot\end{smallmatrix}$ $\begin{smallmatrix}\cdot\\ +\\ \cdot\\ \cdot\end{smallmatrix}$ $\begin{smallmatrix}\cdot\\ \cdot\\ +\\ \cdot\end{smallmatrix}$ $\begin{smallmatrix}\cdot\\ \cdot\\ \cdot\\ +\end{smallmatrix}$ to elements of $\mathbf{A}^{-1}\mathbf{w}(t)$ with support in $[0,T)$ $[0,T)$ $[0,T)$ $[0,\infty)$, we can keep only column $\begin{smallmatrix}+\\ \cdot\\ \cdot\\ \cdot\end{smallmatrix}$ and constrain support only to $[0,\infty)$. Columns 2 through 2^{N-1} on the right can all be discarded as redundant in just this way, as the pattern of $+$ entries in the *label* over each appears shifted up to lead with $+$ in some other *label*. The 2^N rows and $2^{N-1}+1$ remaining columns can then be arranged in increasing order of new scalar row and column labels $\mathbf{x}^T\mathbf{2}$ and $\mathbf{2}^T\boldsymbol{\ell}$ respectively, where binary weight vector $\mathbf{2} = (2^0, 2^1, \ldots, 2^{N-1})^T$ and where $\boldsymbol{\ell} = (\ell_1, \ldots, \ell_N)^T$ is the column-label vector shown above. Finally, let us index the columns $\{\mathbf{c}_i\}$ with the new scalar label and use harmless column operations to replace each $\mathbf{c}_i$ except $\mathbf{c}_0$ and $\mathbf{c}_1$ with $\frac{1}{2}(\mathbf{c}_0 - \mathbf{c}_i)$. The $\{0,1\}$ valued elements then give each column a boolean event-detection character.

The modified model table for a given N, as shown in Fig. 6 for $N = 16$, now incorporates within it the tables for all smaller N. On the right, $h_0(t)$, $h_1(t)$, and $h_3(t)$ are associated with output terms respectively capturing clock-lines generation, LTI response, and the effects of transition asymmetry. Other responses $\{h_i(t)\}$ are ordered by the length of the nonlinear memory involved.

A roundabout general construction here helped justify the table's final form, but starting with appropriately sequenced vector row and column labels $\mathbf{x}^T$ and $\boldsymbol{\ell}$ would certainly expedite a more-direct construction.

4 SUMMARY AND CONCLUSIONS

The model presented here exactly represents any causal, time-invariant nonlinear system that maps the N most-recent binary-data input samples to a real- or complex-valued, continuous-time, analog output. (Using $\{0,1\}$ valued instead of $\{\pm 1\}$ valued input data requires minor changes.) The model is a Wiener-Hammerstein system comprising a simple SIMO tapped delay line, a memoryless nonlinear—all binary in fact—MIMO system, and an LTI MISO system. The constraint length fixes all but the final LTI subsystem, so model fitting or system identification in applications should be relatively simple. The key strength of the model is its separation of constituent waveforms according to the length of nonlinear memory involved. This makes the model's LTI component, in particular, identifiable and separable.

Curiously, the class of nonlinearities modeled is established here to be, to within clock-rate output components, isomorphic to the class of systems in which a binary convolutional coder drives a periodically time-varying linear system with a one-codeword period.

References

[1] K. D. Fisher, J. M. Cioffi, W. L. Abbott, P. S. Bednarz, and C. M. Melas, "An adaptive RAM-DFE for storage channels," *IEEE Trans. Communications*, vol. 39, pp. 1559–1568, Nov. 1991.

[2] Y. Kim and H.-S. Lee, "A decision-feedback equalizer with pattern-dependent feedback magnetic recording channels," *IEEE Trans. Communications*, vol. 49, pp. 9–13, Jan. 2001.

[3] K. O. Andersson, N. U. Andersson, and J. J. Wikner, "Spectral shaping of DAC nonlinearity errors through modulation of expected errors," in *IEEE Int'l Symp. on Circuits and Systems* (Sydney, Australia), pp. 417–420 (vol. 3), May 6–9, 2001.

[4] L. Risbo and H. K. Andersen, "Conversion of a PCM signal into a UPWM signal." International patent WIPO WO97/37433, Australian patent 721526:
http://pericles.ipaustralia.gov.au/aub/pdf/2000/0706/199725672B2/199725672.pdf.